A new laboratory technique for determining the compressional wave properties of marine sediments at sonic frequencies and *in situ* pressures*

Clive McCann[1,2], Jeremy Sothcott[1] and Angus I. Best[1,3]

[1]National Oceanography Centre, University of Southampton Waterfront Campus, European Way, Southampton, Hampshire, SO14 3ZH, United Kingdom.

[2] Professor Emeritus of Geophysics, The University of Reading, Whiteknights, Reading, RG6 2AB, United Kingdom.

[3]Corresponding author email: angus.best@noc.ac.uk

***Presented at the 73rd EAGE Conference & Exhibition, Vienna, Austria, paper number E041.**

ABSTRACT

We describe a new laboratory technique for measuring the compressional wave velocity and attenuation of jacketed samples of unconsolidated marine sediments within the acoustic (sonic) frequency range 1 - 10 kHz and at elevated differential (confining – pore) pressures up to 2.413 MPa (350 psi). The method is particularly well suited to attenuation studies because the large sample length (up to 0.6 m long, diameter 0.069 m) is equivalent to about one wavelength, thus giving representative bulk values for heterogeneous samples. Placing a sediment sample in a water-filled, thick-walled, stainless steel Pulse Tube causes the spectrum of a broadband acoustic pulse to be modified into a decaying series of maxima and minima, from which the Stoneley, and compressional wave, velocity and attenuation of the sample can be determined. Experiments show that PVC and copper jackets have a negligible effect on the measured values of sediment velocity and attenuation which are accurate to better than ± 1.5% for velocity and up to ± 5% for attenuation. Pulse Tube velocity and attenuation values for sand and silty clay samples agree well with published data for similar sediments, adjusted for pressure, temperature, salinity and frequency using standard equations. Attenuation in sand decreases with pressure to small values below $Q^{-1} = 0.01$ (Q greater than 100) for differential pressures over 1.5 MPa, equivalent to sub-seafloor depths of about 150 m. By contrast, attenuation in silty clay shows little pressure dependence and intermediate Q^{-1} values between 0.0206 – 0.0235 (Q = 49 - 43). The attenuation results fill a notable gap in the grain size range of published datasets. Overall, we show that the Pulse Tube method gives reliable acoustic velocity and attenuation results for typical marine sediments.

Keywords: P-waves, velocity, attenuation, marine sediments

INTRODUCTION

Knowledge of compressional (P-) and shear (S-) wave properties of marine sediments at acoustic (sonic) frequencies at appropriate pressures and temperatures can guide the interpretation of shallow, high resolution seismic seafloor surveys, such as those using CHIRP sub-bottom profilers for geotechnical engineering and other applications. This knowledge would also aid our understanding of the reduction in bandwidth of outgoing and returning seismic pulses in deep seismic surveys. Also, measurements at high differential pressure (confining pressure minus pore fluid pressure) are helpful in the interpretation of seismic surveys of deeply-buried sedimentary horizons. Published measurements of these properties can be found at elevated pressures at ultrasonic frequencies in the laboratory (LeBlanc et al, 1994; Buckingham, 2005), and at low effective pressures at kilohertz frequencies in the laboratory (Shumway, 1960), as well as *in situ* measurements on the seafloor (Hamilton, 1972). However, we are unaware of previous laboratory experiments that address the important combination of acoustic (kilohertz) frequencies and high differential pressures for marine sediments.

This paper describes a new laboratory technique for the measurement of P- wave velocity and attenuation of cylindrical samples of unconsolidated sediment (diameter 0.069 m and length up to 0.6 m) within the acoustic frequency range 1 - 10 kHz at differential pressure (here defined as confining pressure minus pore fluid pressure) up to 2.413 MPa (350 psi; all measurements reported here were made using psi). The measurements were made using a Pulse (or Impedance) Tube as shown in Figure 1; it is a water-filled, thick-walled stainless steel tube of internal diameter 0.07 m and length up to 8 m. The temperature and pressure of the water can be varied upwards from 4 °C and up to 2.413 MPa (350 psi), respectively. The tube is insonified by a transducer, located at the base,

giving a usable frequency range of 1 - 10 kHz; the transmitted pulse can be a tone burst, a variable frequency chirp or an impulse. Figure 2 shows example CHIRP and impulse source pulses and their frequency spectra for the water-filled Pulse Tube with and without a sediment sample. There are a number of receiving transducers located along the length of the tube, one of which was used to detect and measure the transmitted signal through the sediment sample. The research was carried out using the Pulse Tubes at various UK government and industry laboratories, where they are normally used for measuring the acoustic properties of sonar materials.

We outline the theory of wave propagation in the Pulse Tube and the modification to the wave field caused by a sediment sample. We describe experiments to validate the measurement technique using standard materials and sand, together with analyses of the acoustic effect of jacketing the sediment. We describe the experimental methods used in the Pulse Tube, the processing and interpretation of the results, and we present example acoustic data for sand and silty-clay samples. The Pulse Tube data are shown to be in excellent agreement with both ultrasonic data and published acoustic data for similar sediments.

THEORY

Low frequency wave propagation in the Pulse Tube

An acoustic waveguide, consisting of a fluid inside a solid cylindrical tube, is a common configuration for measuring the acoustic properties of materials. Sound velocity and attenuation of fluids are measured using samples contained in a solid tube and the acoustic properties of elastic materials terminating the waveguide are measured from their

reflection coefficients. Redwood (1960) showed that the fluid-filled, rigid walled waveguide has an axially-propagating, plane wave mode (the fundamental mode) with a phase velocity equal to the intrinsic sound velocity of the fluid. The wave front is planar and longitudinal. In a waveguide of radius 0.035 m, such as those used in our experiments, no higher order mode propagates at frequencies less than 26 kHz.

When the wall of the acoustic waveguide has a finite shear modulus, a Stoneley wave propagates in the fluid with velocity smaller than that of the compressional wave. Biot (1952) showed, for a borehole with a finite shear modulus wall, that the zero-order acoustic mode propagating in the fluid is a dispersed Stoneley wave and that at low frequencies this is the only wave which can propagate. Figure 8 in Biot's (1952) paper shows that the dispersion of the Stoneley wave is small when the density of the fluid is a small fraction of the density of the material of the borehole wall. For example, the phase velocity of a Stoneley wave at 5 kHz, propagating in a 0.07 m diameter borehole with a density ratio of the fluid to the wall material of 0.4, is only 0.45% greater than that of the long wavelength, asymptotic, constant value. The phase velocity dispersion decreases as the fluid density reduces relative to that of the borehole wall material. Biot (1952) showed that the long wavelength Stoneley wave phase velocity, $V_{Stoneley}$, is given by

$$V_{Stoneley} = \frac{V_{fluid}}{\sqrt{1+\frac{\rho_{fluid}.V_{fluid}^2}{\rho_{tube}.V_{sheartube}^2}}}, \qquad (1)$$

where: V_{fluid} is the acoustic velocity of the fluid; ρ_{fluid} is the density of the fluid; $V_{sheartube}$ is the shear wave speed of the pulse tube material; and ρ_{tube} is the density of the pulse tube material.

Experiments were carried out to determine if equation (1) could be applied to wave propagation in a thick-walled, stainless steel, water-filled tube. The phase velocities of a 5 kHz tone burst Stoneley wave propagating in distilled water at a temperature of 4 ºC and at pressures from 0.345 MPa (50 psi) to 2.413 MPa (350 psi) in a 7.6 m long, thick-walled, stainless steel tube were measured to be 1447.4 ± 0.7 ms^{-1}. Inserting appropriate values ($V_{sheartube}$ = 3200 ms^{-1}; ρ_{tube} = 7740 kgm^{-3}; V_{fluid} = 1467 ms^{-1}; ρ_{fluid} = 1000 kgm^{-3}) into equation (1) gives the long wavelength Stoneley wave velocity of the water in the tube as 1447.5 ms^{-1}, in excellent agreement with the measured value. This agreement shows that equation (1) is applicable to propagation in a fluid within a thick walled, stainless steel tube, and that the velocity dispersion is negligible in the case of the large density contrast between water and steel.

It will be shown below that the useable bandwidth for the acoustic measurements on jacketed sediments in the Pulse Tube is within the range 1 - 8 kHz. Figure 8 in Biot's (1952) paper can be used to show that for a sand sample of density 2000 $kg.m^{-3}$ and Stoneley wave velocity 1750 ms^{-1}, the dispersion at the middle of this frequency range is less than 0.28%. This potential systematic error can be ignored in comparison with the statistical error of the velocity measurements, which is demonstrated below to be between ± 1% and ± 2%. Furthermore, both the internal consistency of the acoustic data described in this paper and their agreement with published data confirm that the Biot (1952) theory of wave propagation in a fluid-filled borehole can be applied to propagation in a thick-walled, high density, stainless steel tube. Below, we show how equation (1) can be used to derive a relationship between the Stoneley wave attenuation of the sediment, measured in the Pulse Tube, and its compressional wave attenuation.

A sediment sample placed in the Pulse Tube causes multiple reflections of the transmitted pulse from its top and base. The amplitude spectrum of the acoustic signal received at a hydrophone above the sample exhibits maxima and minima, caused by constructive and destructive interference at particular frequencies. The frequencies of the maxima enable a wave velocity of the sediment to be measured and the decay of the amplitudes of the maxima enable an attenuation to be estimated.

The response of a sediment sample to the propagating Stoneley wave

We model the response of the sediment sample by considering transmission of an orthogonal plane wave through an infinite plate of finite thickness L and acoustic impedance I_2 (i.e., the product of acoustic velocity and density) immersed in a fluid of acoustic impedance I_1. If the plate is lossless, the inverse complex transmission coefficient of compressional waves through it is given by Kinsler and Frey (1962) as

$$\frac{A_1}{\hat{A}_3} = \frac{(I_1 + I_2)^2 . e^{i.k_2.L} - (I_1 - I_2)^2 . e^{-i.k_2.L}}{4 I_1 . I_2}, \qquad (2)$$

where: A_1 is the amplitude of the input wave; $\hat{A}_3$ is the complex amplitude of the transmitted wave (the hat symbol indicates a complex quantity); k_2 is the wave number in medium 2 (= ω / V_2 where ω is angular frequency); i is the complex operator = $\sqrt{-1}$.

The standard method to include a loss term for the plate is to make k_2 complex. In this case the inverse transmission coefficient has the same form as equation (2) but with

$$\hat{k}_2 = \frac{\omega}{V_2} - \frac{i\omega}{2Q.V_2} \tag{3}$$

and

$$\hat{I}_2 = \rho_2 . \frac{\omega}{\hat{k}_2}, \tag{4}$$

where: V_2 is the absolute value of the velocity of the plate; Q is the quality factor of the plate at angular frequency ω.

This expression was used to calculate theoretical values of the amplitude and phase of the transmission coefficient. When the attenuation coefficient of medium 2 is zero, the amplitude of the transmission coefficient decreases from 1 at zero frequency to a minimum value (which depends on the relative impedance of the two materials) and then increases to 1 at a frequency of $\frac{nV_2}{2L}$ where n = 1, 2, 3 etc. If medium 2 has a finite attenuation, the transmission coefficient at these frequencies is less than one.

Figure 3a shows the theoretical transmission curves for a quartz sand sample of length 0.4 m, compressional wave velocity 1700 ms^{-1}, density 2000 $kg.m^{-3}$ and Q^{-1} = 0.01, 0.02 &

0.04, (quality factors 100, 50 & 25 respectively). We used this model to determine the speed and attenuation of the Stoneley wave propagating through sediment samples.

Wave propagation through sediment samples in the Pulse Tube

Given that the jacketed sediment system measured in the Pulse Tube has a finite shear modulus, we must consider if its measured speed corresponds to a compressional, Stoneley or extensional (Young's Modulus) wave mode. If the sediment container was mounted in air, a Young's Modulus wave, or rod wave, would propagate. If the impedance of the sediment was perfectly matched to that of the water in a tube with walls of infinite rigidity, then a compressional wave would propagate. However, there is an acoustic impedance mismatch between the sediment (3.3×10^6 $kg.m^{-2}.s^{-1}$) and the water (1.5×10^6 $kg.m^{-2}.s^{-1}$).

Dubbleday and Capps (1984) demonstrated theoretically that even a steel rod propagates a compressional wave when contained in a fluid inside a tube with walls of infinite rigidity, provided the ratio of the radius of the tube to the radius of the sample is smaller than 1.001. They showed that a low impedance material, such as the sediment-jacket system, propagates a compressional wave for a radius ratio less than 1.03. The ratio of the radii of tube wall to the container used in our experiments was 1.014, much less than this critical value.

Hence, we conclude that a compressional wave propagates in the sediment-jacket system in a Pulse Tube with walls of infinite rigidity. The finite rigidity of the tube walls modifies this into the Stoneley wave for a sediment-jacket system of low shear modulus,

of which the velocity is about 4 % slower than the equivalent compressional wave, as shown by Biot (1952).

Velocity and attenuation of the jacketed sediment sample

The compressional wave speed of a jacketed sediment sample can be related to its Stoneley wave speed by rearranging equation (1) to give

$$V_{Psj} = \frac{V_{Ssj}}{\sqrt{1 - \frac{\rho_{sj}.V_{Ssj}^2}{\rho_{tube}.V_{sheartube}^2}}}, \tag{5}$$

where: V_{Psj}, V_{Ssj} and ρ_{sj} are the compressional wave velocity, Stoneley wave velocity and density of the jacketed sediment sample respectively; $V_{sheartube}$ and ρ_{tube} are the shear wave velocity and the density of the Pulse Tube respectively.

The compressional wave attenuation of the jacketed sediment sample, expressed as Q_{Psj}^{-1} (where π/Q is the loss per wavelength), can be determined from the measured attenuation of the Stoneley wave of the jacketed sediment Q_{Ssj}^{-1} as follows. Squaring equation (1) and multiplying each side by ρ_{sj}, we obtain

$$\rho_{sj}.V_{Ssj}^2 = \frac{\rho_{sj}.V_{Psj}^2}{1 + \frac{\rho_{sj}.V_{Psj}^2}{\rho_{tube}.V_{sheartube}^2}}. \tag{6}$$

Inverting both sides and multiplying numerator and denominator on the right-hand side by $\rho_{tube}.V_{sheartube}^2$ we obtain

$$\frac{1}{\rho_{sj}.V_{Ssj}^2} = \frac{\rho_{tube}.V_{sheartube}^2 + \rho_{sj}.V_{Psj}^2}{\rho_{tube}.V_{sheartube}^2.\rho_{sj}.V_{Psj}^2}. \quad (7)$$

That is,

$$\frac{1}{\rho_{sj}.V_{Ssj}^2} = \frac{1}{\rho_{sj}.V_{Psj}^2} + \frac{1}{\rho_{tube}.V_{sheartube}^2}, \quad (8)$$

which can be expressed as

$$\frac{1}{M_{Ssj}} = \frac{1}{M_{sheartube}} + \frac{1}{M_{Psj}}. \quad (9)$$

M_{Ssj} is the Stoneley wave elastic modulus of the jacketed sediment sample; M_{Psj} is the compressional wave elastic modulus of the jacketed sediment sample; and $M_{sheartube}$ is the shear wave elastic modulus of the material of the tube wall.

The Pulse Tubes used in our experiments were made from stainless steel, assumed to be lossless. The relationship between the compressional wave attenuation and the Stoneley wave attenuation of the jacketed sediment can be determined by making the elastic moduli complex. Hence, equation (9) becomes

$$\frac{1}{(M_{Ssj}+iM'_{Ssj})}=\frac{1}{(M_{Psj}+iM'_{Psj})}+\frac{1}{M_{sheartube}}, \qquad (10)$$

where: M_{Ssj} and M'_{Ssj} are the real and imaginary parts of the complex Stoneley wave elastic modulus of the jacketed sediment; M_{Psj} and M'_{Psj} are the real and imaginary parts of the complex compressional wave elastic modulus of the jacketed sediment; and $M_{sheartube}$ is the shear wave elastic modulus of the material of the tube wall. Multiplying the numerators and denominators of equation (10) by their complex conjugates, assuming terms in M'^2 are small and can be ignored, equating the imaginary parts (which define the attenuation properties), making use of the relationship that Q^{-1} is equal to the ratio of the imaginary part to the real part of the complex modulus, and substituting in for M_{Psj} in terms of M_{Ssj} and $M_{sheartube}$ from equation (9), we obtain the following equation.

$$\frac{1}{Q_{Psj}}=\frac{1}{Q_{Ssj}}.\frac{M_{sheartube}}{(M_{sheartube}-M_{Ssj})}, \qquad (11)$$

where Q_{Psj}^{-1} and Q_{Ssj}^{-1} are, respectively, the compressional and Stoneley wave attenuations in the jacketed sediment sample. For typical values of the shear modulus of the stainless steel tube wall and of the Stoneley wave modulus of the sediment, the compressional wave attenuation of the sediment is about 5 % greater than the measured Stoneley wave attenuation.

INITIAL INVESTIGATIONS

Nylon rod experiment

The concept of using the Pulse Tube to determine acoustic properties from the transmission coefficient spectra was tested using a nylon (TECAMID 66) cylinder and a clean, well-sorted quartz sand.

The initial experiments were carried out using an 8 m long Pulse Tube at the laboratories of GEC-Marconi at Templecombe in Dorset, England. The nylon cylinder (0.2014 m long and 0.069m diameter) sample was carefully degreased and lowered on a thin nylon line to hang just below a mid-tube hydrophone. The water pressure was kept fixed at 1.379 MPa (200 psi) for all the measurements to ensure that the spectrum of the source pulse remained constant; this spectrum was measured regularly throughout the experiments with no sample in the tube.

In our initial experiments, we used a tone burst pulse (a flat-topped, single frequency sinusoid) to excite the transducer at the base of the Pulse Tube. It was varied in 0.5 kHz frequency steps from 0.5 - 10 kHz and the signal was measuring at a hydrophone set in the wall of the Pulse Tube at 4.2 m above the base. The duration of the tone burst was carefully adjusted to ensure that there was no interference between the direct pulse and subsequent reflections from the top and base of the Pulse Tube. The transmission coefficient of the sample at each frequency was determined by dividing the amplitudes of the same phase points on each tone burst, measured in the presence and absence of the sample respectively. Figure 3b shows an example transmission coefficient spectrum for the nylon rod (Dataset 17/10/94/09) at a confining pressure of 1.379 MPa (200 psi), together with the best-fit theoretical solution in the bandwidth 1 - 8 kHz; the transmission coefficient spectrum is unstable outside this frequency range. Table 1 gives the Stoneley

wave velocity and attenuation Q^{-1} for this solution as 2400 ± 25 ms^{-1} and 0.0067 ± 0.0038 (Q = 150) respectively with an R^2 value of 0.92, showing that 92% of the variance of the experimental data is accounted for by the theoretical model.

The error bars were determined from the range of velocities and attenuations obtained when the sum-of-squares of the residuals was allowed to increase by 10% from the best-fit solution. The Stoneley wave values were converted into the equivalent P-wave results using equations (5) and (11): the P-wave velocity and attenuation of the nylon cylinder were 2500 ± 25 ms^{-1} and 0.0071 ± 0.0038 (Q = 141) respectively (see Table 1).

The accuracy of these data was checked by comparing the equivalent P-wave velocity calculated at 0.5 MHz using equation (12) (from Kolsky, 1956) with that measured directly using ultrasonic transducers (see Table 1).

$$V_p(f_1) = V_p(f_2).\left[1 + \frac{1}{\pi Q_{Ps}}.\log_e\left(\frac{f_1}{f_2}\right)\right], \qquad (12)$$

where $V_p(f_1)$, $V_p(f_2)$ are the nylon compressional wave velocities at frequencies f_1 and f_2 respectively, and Q_{Ps}^{-1} is the nylon attenuation in the frequency range from f_1 to f_2. The attenuation was assumed to be constant over the frequency range from 4.5 kHz to 0.5 MHz and its error bar was used to determine the final accuracy of the predicted high frequency velocity. The predicted velocity at 0.5 MHz is 2527 ± 29 ms^{-1}, in good agreement with the directly determined ultrasonic value of 2540 ± 19 ms^{-1}.

This result gives confidence in the Pulse Tube transmission coefficient technique for measuring the acoustic properties of test materials.

Sand experiments

Pulse Tube measurements were made on clay-free, quartz (Leighton Buzzard) sand shown in Figure 4a with physical and chemical properties given in Table 2. Cylindrical containers were constructed from PVC and copper to hold the sand within the Pulse Tube as shown in Figure 4b.

The PVC container was constructed using standard drainpipe, 0.069 m diameter, initially 0.2 m long and with a wall thickness of 0.185 cm. The acoustic impedance of the PVC is very similar to that of water saturated sand, about 3.2×10^6 $kg.m^{-2}.s^{-1}$. The lower end of the PVC container was sealed by a thin rubber membrane of thickness 0.15 cm, which enabled the external confining pressure to be applied to the sediment. The top end of the container was sealed by a moveable Perspex piston and "O" ring, allowing the sediment to compact in response to the external confining pressure. A pressure port was located in the centre of the piston, connected via thick-walled nylon pressure tubing to valves set within the top cap of the Pulse Tube. The latter enabled the pore fluid pressure within the sand to be varied independently of the confining pressure (see Figure 4c).

The following sand sample preparation procedure was used to ensure full water saturation. The sand and distilled water were placed in a desiccator attached to a modified bottle shaker, and left under vacuum and shaken for eight hours. A rubber tube from the outlet at the base of the vacuum desiccator was then lowered beneath the surface of de-

aired water in the PVC sample container (jacket). The vacuum was released and the sand was allowed to tumble into the sample container. When the sample container was almost full, the rubber tube was removed and the Perspex piston was inserted to fit flush against the flat surface of the sand. The sand sample was placed in a pressure vessel and taken to a confining pressure of 3.5 MPa with the pore fluid vented to atmospheric pressure. This procedure pre-compacted the sand before it was used in the Pulse Tube, and also pre-tested the container to reduce the risk of failure within the Pulse Tube.

The copper sample container (jacket) consisted of a sheet of 0.013 cm thick copper foil rolled onto a cylindrical former of diameter 0.069 m. Copper caps were soldered to both ends of the copper cylinder, the top cap having a fluid entry port in its centre. The sand was run into the copper container as previously described for the PVC container. The container was pressurised to 5 MPa with the pore fluid vented to atmospheric pressure, forcing the thin copper walls into close contact with the sand.

The experiments with the sand-filled containers were carried out in the 8 m long Pulse Tube at the GEC-Marconi Laboratories. Each sample container was carefully degreased, then a pore-fluid pipe and nylon safety line were attached to the top of the container, which was lowered to hang just below a mid-tube hydrophone. The water pressure in the Pulse Tube was held at 2.413 MPa (350 psi) while the pore fluid pressure was varied to obtain differential pressures between 0.345 MPa (50 psi) and 2.068 MPa (300 psi). The initial experiments were carried out using a tone burst pulse, exactly as described for the nylon cylinder above. The transmission coefficient of the sample at each frequency was

determined by dividing the amplitudes of the received pulse measured with and without the sample in the tube respectively.

Figure 5a shows the transmission coefficient spectrum with two maxima and two minima for a sand sample in a copper jacket, of length 0.2030 m (Dataset N/17/10/94/08), at a differential pressure of 1.379 MPa (200 psi). The best fit theoretical model over the frequency bandwidth from 0.94 - 8.44 kHz has a Stoneley wave velocity of 1780 ± 29 ms^{-1} and attenuation Q^{-1} of 0.016 ± 0.010 (Q = 60). The calculated R^2 value of 0.71 shows that 71% of the variance of the experimental data is accounted for by the theoretical model.

Having established that useful results could be obtained, the measurement technique was refined by driving the source transducer with a CHIRP pulse which increased in frequency from 0.5 - 10 kHz over a pulse length of just over 4 ms (see Figures 2a & c). The acoustic signal was stacked 10 times to improve signal-to-noise ratio before calculating the transmission coefficient spectrum from the signal.

We decided to increase the length of each sediment sample to 0.4 m to both increase the number of transmission coefficient maxima (to four) and to increase the decay rate of the spectrum, thus enabling the Stoneley wave velocity and attenuation of the sample to be determined more precisely. Figure 5b shows example data for the sand in a 0.385 m PVC container at 2.068 MPa (300 psi) differential pressure (Dataset 6/6/95/006). The noisy low frequency part of the spectrum is caused by interference between the signal and later arrivals reflected from the top and bottom of the Pulse Tube. There are three clear

maxima with part of a third minimum appearing before the spectrum starts to decay significantly at frequencies above 7.4 kHz. This behaviour of a noisy low frequency region and an unstable high frequency region limited the analysis of many of the transmission spectra to a bandwidth between 1.0 - 8.0 kHz. The best fit theoretical model over the frequency bandwidth from 1.4 - 7.4 kHz has a Stoneley wave velocity of 1760 ± 15 ms^{-1} and attenuation Q^{-1} of 0.00667 ± 0.00340 (Q = 150). The R^2 value of 0.90 shows that 90% of the variance of the experimental data is accounted for by the theoretical model. Equations (5) and (11) were used to convert the velocity and attenuation to their equivalent P-wave values of 1825 ms^{-1} and 0.00717 (Q = 140) respectively.

Sediment jacket corrections

Corrections for the effects of the copper and PVC containers were investigated. Gemant (1940) published a theoretical analysis of the effect of the jacket in a resonant bar system given by

$$V_{Ps} = \sqrt{\frac{m_{sj}.V_{Psj}^{\ 2} - m_j.V_{Pj}^{\ 2}}{m_s}} \tag{13}$$

and

$$\frac{1}{Q_{Ps}} = \frac{\left(\frac{m_{sj}.V_{Psj}^{\ 2}}{Q_{Psj}} - \frac{m_j.V_{Pj}^{\ 2}}{Q_{Pj}} \right)}{m_s.V_{Ps}^{\ 2}}, \tag{14}$$

where: m_s, m_{sj} and m_j are the masses of the sediment, the sediment-jacket combination, and the jacket respectively; V_{Ps}, V_{Psj} and V_{Pj} are the compressional wave velocities of the sediment, the sediment-jacket combination and the jacket; and Q_{Ps}, Q_{Psj} and Q_{Pj} are the compressional wave quality factors of the sediment, the sediment-jacket combination and the jacket.

Book values of the P-wave velocity (4759 ms^{-1}) and attenuation (zero) of copper were used in equations (13) and (14) to determine the corrections for the copper jackets. The P-wave velocity and attenuation of PVC were measured on a rod of length 0.4147 m in the Pulse Tube (Table 1) to be 2309 ± 25 ms^{-1} and 0.0310 ± 0.0042 (Q = 32) respectively. As a check, the equivalent P-wave velocity at 0.5 MHz was calculated from the Pulse Tube value assuming a linear variation of Q^{-1} from 0.0310 at 5.3 kHz to 0.0075 at 0.35 MHz (Kaye and Laby, 1995). A simple attenuation/dispersion model was designed for this calculation, consisting of four parallel Maxwell elements (each comprising an elastic spring in series with a viscous dashpot) in parallel with a fifth elastic spring. Kolsky (1953) evaluated the frequency response of this type of mechanical dissipation model. The characteristic frequencies of the four elements were 2 kHz, 20 kHz, 100 kHz and 1 MHz respectively. The attenuation response of the model was adjusted to equal the known experimental variation of Q^{-1} with frequency, from which the consequent frequency dispersion of the elastic modulus (and hence the change in P-wave velocity) was determined. Table 1 shows that there is excellent agreement between the frequency-corrected Pulse Tube P-wave velocity (2365 ± 29 ms^{-1}) and the value determined by direct ultrasonic measurement (2363 ± 19 ms^{-1}).

The P-wave velocity and attenuation data for the sand as a function of differential pressure are shown respectively in Figures 6a and 7a, uncorrected for the acoustic effects of the PVC and copper jackets, and in Figures 6b and 7b, corrected for the effects of the containers using equations (13) and (14) respectively. There is excellent agreement between the uncorrected velocities, but the jacket-corrected velocities are significantly different; the corrected velocities for sand in a copper jacket are physically unrealistic, being significantly lower than the velocity in water. Similarly, the jacket-corrected attenuations for sand in a copper jacket are significantly different to those for sand in a PVC container.

It was concluded that application of the jacket correction equations (13) and (14) gives an increased discrepancy between the PVC jacket and the copper jacket results for sand. In reality, the jacket material seems to have little influence on the measured values of the compressional wave velocity and attenuation of the sand, as shown in Figures 6a and 7a. Therefore, we decided not to apply jacket corrections for the experiments on silty-clay sediments described below.

Accuracy of the sand acoustic data

The noisy low frequency region of the transmission coefficient spectra, arising from reflections from the top and base of the Pulse Tube, and the consistently unstable high frequency region above about 8.4 kHz, limited the analysis of all spectra to a bandwidth of 1.0 - 8.0 kHz. Analysis of Figure 8 in Biot's (1952) paper indicates that the systematic error arising from equation (5) to determine the sediment compressional wave velocity

from the measured Stoneley wave velocity, under the assumption that the latter is actually the long-wavelength asymptotic value, is less than 0.28% at the mid-spectral frequency. Analysis of the variance of the data for the sand, for both the PVC and copper jackets, showed that the accuracy of P-wave velocity and attenuation (Q_p^{-1}) are ± 1 % and ± 0.0036 (average) respectively.

Variation of attenuation and velocity with pressure for sands

Figures 8a and b show the variation of compressional wave velocity V_{Ps}, and attenuation Q_{Ps}^{-1}, respectively for sand versus differential pressure P_d for the frequency range 1.5 - 8.2 kHz, and 1.5 – 8.0 kHz, respectively at a temperature of 4 ºC. The linear least squares regression equations representing these statistical relationships are for velocity

$$V_{Ps} = (87 \pm 10).P_d + (1621 \pm 13), \quad (15)$$

(R^2 = 0.91, F = 72),

and for attenuation at differential pressures less than 1.5 MPa

$$Q_{Ps}^{-1} = (0.0260 \pm 0.0038) - (0.0133 \pm 0.0035).P_d , \quad (16)$$

(R^2 = 0.62, F = 9.0, P_d < 1.5 MPa).

The R^2 and F values indicate the relationships for velocity and attenuation are significant at the 99% and 95% confidence levels, respectively. Note that there were insufficient data to obtain a statistically significant non-linear trend for attenuation. However, the average value of Q_{Ps}^{-1}, determined from the three data points at differential pressures greater than 1.5 MPa in Figure 8b, is 0.00783 ± 0.00055 (Q = 128). Fitting a linear

regression to the data for differential pressures between 0 - 1.5 MPa gives the statistical relationship in equation (16).

Comparison of the sand results with published data

Shumway (1960) published P-wave velocities and attenuations for seafloor sands, silts and clays, measured in the laboratory at ambient pressure, sonic frequencies and room temperature. The P-wave velocities of ten of Shumway's sand samples are given in Table 3; we converted them to their equivalent values at 5 kHz, 4 ºC, 0 ppt salinity and 2.413 MPa (350 psi) pore water pressure and zero differential stress for comparison with the Pulse Tube sand acoustic data. The P-wave velocity V_p of the saturated sands in Table 3 is given by

$$V_p = \sqrt{\frac{K^* + \frac{4}{3}\mu}{\rho}}, \tag{17}$$

where K^*, μ and ρ are the bulk modulus, the shear modulus and the wet density of the sand respectively. Briggs (1991) gave shear wave velocities of 83 ms^{-1} and 78 ms^{-1} for sands of porosities 0.39 and 0.38 respectively, corresponding to an average shear modulus of 17.2 MPa. Combining this value with the measured values of V_p and ρ given in Table 3 enabled us to calculate K^* for each sand. The variation of K^* with temperature and pore-water salinity was calculated using Gassmann's equation (Gassmann, 1951; Wang, 2000)

$$K^* = K_d + \frac{\left(1 - \frac{K_d}{K_m}\right)^2}{\frac{\varphi}{K_f} + \frac{1-\varphi}{K_m} - \frac{K_d}{K_m^2}}, \tag{18}$$

where: K^* is the bulk modulus of the fluid saturated sand; K_f is the bulk modulus of the pore fluid at temperature T and salinity S; K_d is the "frame" bulk modulus of the sand; K_m is the bulk modulus of the quartz sand grains (38 GPa); and φ is the fractional porosity of the sand. The variables μ, K_d, K_m and φ are independent of salinity and temperature.

The variation of the bulk modulus of the pore water K_f with density ρ and compressional wave velocity V_p, both functions of temperature T (ºC), salinity S (ppt or parts per thousand) and pressure P (MPa) are given by

$$K_f(T,S,P) = \rho(T,S,P) \times V_p^2(T,S,P), \quad (19)$$

and

$$V_p(T,S,P) = 1449.2 + 4.6T - 0.055T^2 + 0.00029T^3 + (1.34 - 0.01T)(S-35) + 1.63P \quad (20)$$

.

Equation (20) was taken from Clay and Medwin (1977).

We adjusted the frame bulk modulus K_d for each sand until the predicted value of K^* equalled the experimental value from Table 3, using values of K_f appropriate for the temperature, salinity and pore water pressure of the sand sample. We used the values of K_f for pore water at 4 ºC, 0 ppt salinity and pore water pressure of 2.413 MPa (equivalent to 0 MPa differential pressure) in equations (17 – 20) to calculate the equivalent sand bulk modulus and P-wave velocity under the conditions of the Pulse Tube sample measurements. P-wave velocity was adjusted from the frequency used by Shumway (1960) to the mean Pulse Tube

frequency of 5 kHz using the published values of attenuation, assumed constant over the frequency range in equation (12).

Table 3 shows that the mean P-wave velocity of the ten sands of average porosity 0.383 ± 0.014 in Shumway's dataset, amended to the condition of the Pulse Tube measurements at zero differential stress, is 1607 ms^{-1}, with a standard error of the mean of ± 8 ms^{-1} (sample standard deviation ÷ √(number of samples), in reasonable agreement with the ambient pressure intercept of the sand used in the Pulse Tube experiments of 1621 ± 13 ms^{-1} (see Figure 8a). The lower mean velocity of Shumway's sands occurs because their mean porosity is 8.8% greater than that of the quartz sand measured in the Pulse Tube.

Table 3 shows also that the mean P-wave attenuation Q^{-1} of the ten sands from Shumway's dataset is 0.0244 (Q = 41) with a standard error of the mean of ± 0.0024, in excellent agreement with the ambient pressure intercept of the attenuation data in Figure 8b of the sand measured in the Pulse Tube of 0.0260 ± 0.0038 (Q = 38.5).

We conclude that the P-wave velocity and attenuation of clean, well-sorted sand that we measured in the Pulse Tube are consistent with data for similar porosity sands published by Shumway (1960). The agreement of the attenuation data for the jacketed sand with those of Shumway demonstrates the losses are due to propagation in the bulk sediment rather than an artefact caused by fluid flow at the surface of the sample, as can occur in unjacketed samples (White, 1985). The data show that the compressional wave attenuation of the sand decreases rapidly with increasing differential pressure or increasing depth of burial beneath the seafloor. The higher pressure measurements indicate that, at depths of burial greater than about 150 m, the compressional wave attenuation of the sand is about one quarter of its value

at the seafloor. Hence, for sands at least, it is the very shallow sediments that are responsible for the large high-frequency loss suffered by seismic pulses transmitted downwards and reflected upwards through the seafloor.

VELOCITY AND ATTENUATION OF SILTY-CLAY SEDIMENTS

Sediment samples

Silty-clay sediment sub-samples were taken from cores collected on the UK continental shelf by the British Geological Survey. The sediments were collected in clear plastic tubes 3 m long, 0.085 m internal diameter and 0.09 m external diameter. The cores were cut into three equal lengths for transportation and storage and sealed with end caps, wax and tape. The ultrasonic compressional wave velocities of the sediments were measured across the core diameters on board the ship for assessment of any subsequent disturbance. On receipt of the cores in our laboratory, their states of saturation were estimated by both visual examination and by repeat measurements of their ultrasonic compressional wave velocities. Cores which appeared to be fully saturated, or could be re-saturated, were subsequently sub-sampled for measurement of their sonic properties in the Pulse Tube. Geotechnical properties were determined for all of the sediment cores.

Sub-sampling procedure

Experiments showed that the quality of the acoustic data obtained for silty clays in the Pulse Tube was critically dependent on the material used for jacketing the samples. These sediments, when jacketed in PVC, gave unstable transmission coefficient spectra. Jacketing the sediment with thin copper enabled stable, repeatable and

accurate compressional wave data to be obtained, the copper jackets having insignificant effects on either the measured velocity or attenuation.

Each copper jacket was manufactured by rolling a copper sheet on to a mandrel of diameter 0.068 m. The longitudinal seam was soldered then a copper disc, pierced with a pore-fluid port, was soldered to seal one end of the jacket (Figure 9a). The copper jacket was placed inside a steel tube (wall thickness 1.5 mm) with about 1 cm of copper extending beyond the end, which was then cut into strips that were bent over to lie flush along the outside of the steel tube (Figure 9b). The principle criteria in sub-sampling the sediment from the original cores into the copper jackets were to maintain full saturation of the sub-sample and to minimise its disturbance. The seafloor core was set up vertically and ultrasonic measurements of compressional wave velocity were made across the diameter. The end cap was carefully removed to expose the sediment, which was photographed (Figure 9e).

The composite copper/steel tube was then pushed into the sediment core, taking great care to ensure that it remained vertical, until sediment emerged from the pore fluid port. This port was then sealed and the steel/copper/sediment sub-sample freed from the original core. The sub-sample was inverted and about 1 cm of sediment removed. The top face of the core was carefully flattened, the wall of the copper jacket was degreased with acetone, then a rubber diaphragm (thickness 1.5 mm) was placed on top of the prepared face. A silicone sealant was extruded around the perimeters of the rubber diaphragm and the copper jacket, and carefully moulded into place with a

smooth spatula (Figure 9c**)**. The sealant cured in about 24 hours. The final length of each sample was about 0.4 m.

The copper jacketed sediment was removed from its steel housing and, after cleaning, was pressurised to 3.5 MPa to check the integrity of the rubber diaphragm. Ultrasonic velocity measurements were again made across the diameter of the sediment sample. Figure 9d shows the copper jacketed sediment in its final form. During the sub-sampling process the weights of the copper jacket, the rubber diaphragm, the silicone sealant and the sediment-filled container were measured so that the average wet density of the sediment could be determined. The grain size distributions of the sediments were determined using a laser granulometer. The samples were stored at 4 °C.

Pulse Tube acoustic measurements

We conducted the acoustic measurements on the copper-jacketed silty-clay sediments in a 4.267 m Pulse Tube located in a UK government laboratory. An impulse acoustic source was generated at the transducer at the base of the Pulse Tube (see Figures 2b & d). The impulse was recorded using the hydrophone set in the wall at 1.59 m below the Pulse Tube top, with the water at a pressure of 2.413 MPa (350 psi). The water pressure was kept fixed at this value for all the subsequent measurements of the sediment samples to ensure that the spectrum of the source pulse remained constant. The water temperature was maintained at 6 °C. The samples were carefully degreased. A pore-fluid pipe and nylon safety line were attached to the top of the copper sleeve. As the sediment was inserted into the Pulse Tube, any air trapped below its base by

the overhang of the walls was carefully removed with a syringe. The sediment tube was lowered to a depth of 2.25 m in the 4.267 m Pulse Tube, to hang well below the top hydrophone. The acoustic signal was stacked 10 times to improve the signal-to-noise ratio before it was used to calculate the transmission coefficient spectrum.

The transmission coefficient spectra obtained for silty-clay sediment samples in the first experiments commonly showed a significant interference trough at about 6 kHz. This was found to be due to air or free water trapped between the sediment base and the rubber diaphragm; bleeding off the air with a hypodermic syringe significantly reduced this interference effect. Measurements were made with the sediment pore fluid pressure at 0.345 MPa (50 psi) and 1.724 MPa (250 psi) respectively, that is at differential pressures of 2.068 MPa (300 psi) and 0.689 MPa (100 psi). The spectra were analysed by comparison with theoretical transmission coefficient data as described above. A typical transmission coefficient spectrum for a silty clay (sample 206C3) is shown in Figure 10 with its best fit theoretical spectrum in the bandwidth 1.4 - 7.8 kHz.

Accuracy of the acoustic data for silty clays

Sample 206B3LH was measured independently on two separate occasions in the Pulse Tube, at a differential pressure of 2.068 MPa (300 psi). The values of P-wave velocity were 1572 ms^{-1} and 1607 ms^{-1}; the P-wave attenuations were 0.0252 (Q = 39.7) and 0.0260 (Q = 38.5), indicating excellent repeatability of the experimental data and of the modelling technique.

The Stoneley wave velocity and attenuation of Sample 206C3 at a differential pressure of 2.068 MPa (300 psi) in Figure 10 were 1425 ms^{-1} and 0.0227 (Q = 44) respectively; the R^2 value of 0.93 shows that, in the bandwidth 1.4 - 7.8 kHz, 93% of the variance of the experimental data is accounted for by the theoretical model. Allowing the sum-of-squares of the residuals to increase by 10% indicated that the error bars for the velocity and attenuation were ± 17 ms^{-1} (± 1.2 %) and ± 0.0011 (± 5 %) respectively. A similar assessment of the error bars for all of the silty clay samples indicated that the average error bar for the Stoneley wave velocities was ± 21 ms^{-1} (± 1.5 %). The error bar for the Q^{-1} data is a function of the absolute value of the attenuation. It varies from ± 5 % for high attenuation samples (Q^{-1} = 0.04; Q = 25) to ± 50 % for low attenuation (Q^{-1} = 0.007; Q = 143).

Compressional wave velocity and attenuation of silty clays

Table 4 shows the geotechnical and the acoustic properties, determined at two differential pressures at sonic frequency in the Pulse Tube, and at ambient pressure at ultrasonic frequency, for nine silty clay samples. For six samples (206C3, 241A3LH, 240A3LH, 240A3UH, 206B3LH and 206C3) there are data for two differential pressures, 0.689 MPa (100 psi) and 2.068 MPa (300 psi). These samples exhibit intermediate attenuations with a mean Q_p^{-1} = 0.0206 ± 0.00235 (Q_p = 48.0 ± 5.5) at 0.689 MPa (100 psi) and a mean Q_p^{-1} = 0.0235 ± 0.00332 (Q_p = 43 ± 6.1) at 2.068 MPa (300 psi) (Student-T value for these data is 1.28 compared to $T_{95\%,10}$ of 1.8125). They show small changes in P-wave velocity with increasing pressure: average at 0.689 MPa (100 psi) = 1476.4 ± 15.7 ms^{-1}; average at 2.068 MPa (300 psi) = 1474.9 ± 14.7 ms^{-1}. We concluded that the silty clay samples showed no significant change in acoustic properties with increasing differential pressure, at least within the range of

pressures and within the duration (a few hours) of our experiments. There are three samples (240B3, 234B3UH, 241A3UH) for which there are data only at a differential pressure of 2.068 MPa (300 psi). These exhibit the intermediate attenuation ($Q_p = 45$) characteristic of the group of six samples.

The data for all the samples at both differential pressures were combined for comparison with the ambient pressure ultrasonic measurements on the same cores, and with published data for similar porosity sediments. The compressional wave velocities of the silty clays, measured at 4 ºC and 5 kHz in the Pulse Tube, were adjusted to a temperature of 20 ºC, to a frequency of 500 kHz and to the appropriate pore water pressure from 0.345 MPa (50 psi) and 1.724 MPa (250 psi) to 0 MPa using equations (12) & (17 – 20). The frequency correction in equation (12) assumes that the attenuation values determined from the Pulse Tube are constant over the whole frequency range. Figure 11 shows the ratios of the ultrasonic to the adjusted Pulse Tube P-wave velocities: the means of the ultrasonic and adjusted Pulse Tube P-wave velocities are 1560.7 ± 17.8 ms^{-1} and 1563.8 ± 7.0 ms^{-1} respectively, an average ratio of ultrasonic to adjusted Pulse Tube P-wave velocity of 0.998.

Table 5 shows acoustic and geotechnical data at ambient pressure, sonic frequencies and room temperature published by Shumway (1960) for twelve seafloor silty clays of similar porosities to the samples measured in the Pulse Tube. These P-wave velocities were converted to their equivalent values at 5 kHz and 6 ºC, and for a change in the pore water pressure from 0 MPa to the average pore water pressure of 1.0345 MPa (150 psi) using equations (12) & (17 – 20) for comparison with the Pulse Tube acoustic data. The mean

of the adjusted P-wave velocities of Shumway's samples is 1469.4 ± 3.2 ms^{-1}, in excellent agreement with the mean P-wave velocity of the Pulse Tube samples of 1468.0 ± 9.4 ms^{-1}.

Figure 12 shows P-wave attenuation Q_p^{-1} for the silty clays measured in the Pulse Tube at effective pressures of 0.689 MPa (100 psi) and 2.068 MPa (300 psi) within the frequency range 1 - 8 kHz plotted against mean grain size (log scale) together with the *in situ* data of Hamilton (1972). Hamilton's data are in the sonic frequency range and are for zero effective pressure (seabed). The Pulse Tube attenuation data fit well with Hamilton's published results and they add a significant number of data points in a grain size range which was previously under-represented.

The Pulse Tube acoustic data show the relatively low P-wave attenuation and low P-wave velocities expected for silty clay samples. The data show insignificant variation with differential pressure and the average values are in good agreement with ambient pressure ultrasonic data adjusted for frequency, temperature and pore fluid pressure, and with Shumway's laboratory data. The attenuation data also agree well with Hamilton's seafloor data. This agreement gives confidence that the Pulse Tube measurement technique is reliable and accurate for copper-jacketed, silty-clay sediments at sonic frequencies. The silty clay data confirm that the sediment jackets have a negligible effect on the measured compressional wave values, similar to the sand results.

CONCLUSIONS

We have presented a new laboratory technique for measuring the acoustic properties of unconsolidated marine sediment samples at combined elevated pressures up to 2.413 MPa (350 psi) and acoustic (sonic) frequencies in range 1 – 10 kHz. A particular advantage of the Pulse Tube method is that it uses sediment samples about a wavelength long; hence, they can contain heterogeneities of a similar size to those found in the Earth, which is important for attenuation studies. This new measurement capability offers significant opportunities for future studies of marine sediment acoustic properties directly relevant to high resolution, seafloor seismic geotechnical surveys.

We have demonstrated that it is possible to obtain accurate and repeatable measurements of velocity and attenuation (better than ± 1.5% for velocity, and as low as ± 5% for attenuation) using standard acoustic pulse tubes, novel sample jacketing and preparation procedures and theory for converting measured Stoneley wave values to the desired compressional wave values. Our Pulse Tube results for sand and silty clay sediments agree closely with published datasets, once adjusted to equivalent conditions of pressure, temperature, pore fluid salinity and measurement frequency using standard equations.

We have shown that PVC and copper jackets have a negligible effect on the acoustic properties measured in the Pulse Tube. For water saturated sands, P-wave attenuation decreases with pressure up 2.413 MPa (350 psi) from intermediate to low values; the average attenuation at seafloor pressures is 0.026 (Q = 38), decreasing to 0.0078 ± 0.00055 (Q = 128) at differential pressures above 1.5 MPa, i.e. greater than about 150 m below the seafloor. For water saturated silty clays, attenuation shows intermediate values between 0.0206 – 0.0235 (Q = 48 – 43) which do not change significantly with pressure.

The new attenuation data fill a significant gap in the grain size range of previously published values for marine sediments.

ACKNOWLEDGEMENTS

This work was supported by the former Defence Research Agency of the United Kingdom. We thank the staff of various Government and industry scientific laboratories for allowing us access to a number of Pulse Tubes during the course of this research. Thanks to Dr. Ian Stevenson for permission to use Figure 1. We are grateful to Maxim Lebedev and Jim Spencer for their helpful and constructive reviews of the paper.

REFERENCES

Biot, M.A. 1952. Propagation of elastic waves in a cylindrical bore containing fluid. *Journal of Applied Physics* **23**, 997-1005.

Briggs K.B.1991, Comparison of measured compressional and shear wave velocity values with predictions from Biot theory. In Shear waves in marine sediments; Hovem J.M., Richardson M.D. and Stoll R.D., Editors. Kluwer Academic Publishers, Dordrecht, 121-130.

Buckingham M.J. 2005. Compressional and shear wave properties of marine sediments: Comparisons between theory and data. *Journal of the Acoustical Society of America* **117**, 137-152.

Clay C.S. and Medwin H. 1977. *Acoustic Oceanography*. John Wiley and Sons, New York.

Dubbleday P.S and Caps R.N. 1984. Interpretation of sample wave speed measured in an impedance tube. *Journal of the Acoustical Society of America* **76**, 964-967.

Gassmann F. 1951. Uber die Elastizitat poroser Medien. Vieteljahrsschrift der Naturforschenden Ges., Zurich, 96, 1-23.

Gemant A. 1940. The measurement of solid friction of jackets. *Journal of Applied Physics* **11,** 647-653.

Hamilton E.L. 1972. Compressional wave attenuation in marine sediments. *Geophysics* **37**, 620-646.

Kaye, G.W.C. & Laby, T.H. 1995. *Tables of physical and chemical constants*. Longman. 611pp.

Kinsler L.E. and Frey A.R. 1962. *Fundamentals of acoustics*. John Wiley and Sons, New York, 521pp.

Kolsky H. 1956. The propagation of stress waves in viscoelastic solids. *Physics Magazine* **1**, 693-710.

LeBlanc L.R., S. Panda and S.G.Schock 1992. Sonar attenuation modelling for classification of marine sediments. *Journal of the Acoustical Society of America* **91**, 116-126.

Redwood M. 1960. Mechanical waveguides. Pergamon Press, London, 300pp.

Shumway G. 1960. Sound speed and absorption studies of marine sediments by a resonance method. *Geophysics* **25**, 451-467.

Sutton, G.H., Berckhemer, H. & Nafe, J.E. 1957. Physical analysis of deep sea sediments. *Geophysics* **22**, 779-812.

Wang Z. 2000. The Gassmann Equation revisited: comparing laboratory data with Gassmann's predictions. Pp 8-23 in "Seismic and acoustic velocities in reservoir rocks, Volume 3. Recent Developments". Wang Z. and Nur A. Editors. Geophysics Reprint Series, 19, Society of Exploration Geophysicists, 633pp.

White J.E. 1985. Biot-Gardner theory of extensional waves in porous rods. Geophysics, 51, 742-745.

Figure captions

Figure 1. Schematic diagram of the acoustic Pulse Tube.

Figure 2. Oscilloscope screen images of a) CHIRP and b) impulse source pulses. Power spectra of the c) CHIRP and d) impulse sources pulses with and without a sample in the Pulse Tube.

Figure 3. a) Theoretical transmission coefficient spectra for a quartz sand of length 0.4 m, Stoneley wave velocity 1700 $m.s^{-1}$ and density 2000 $kg.m^{-3}$. b) Experimental transmission coefficient spectrum for a 0.2014 m nylon cylinder (Dataset 17/10/94/09) at a confining pressure of 1.379 MPa (200 psi), with the best-fit theoretical solution (solid line) in the bandwidth 1 - 8 kHz. The Stoneley wave velocity and attenuation (Q^{-1}) for this solution (R^2 =0.92) are 2400 ± 25 ms^{-1} and 0.0067 ± 0.0038 (Q = 150) respectively.

Figure 4. a) Photograph of typical grains of the well-sorted, quartz (Leighton Buzzard) sand of mean diameter 2 mm used to test the Pulse Tube measurement technique. b) Various samples prepared for the Pulse Tube. From left to right: three containers of sediment with jackets made of PVC (0.2 m), copper (0.2 m) and copper (0.4 m), a solid cylinder of PVC (0.4 m), a PVC jacketed sediment (0.4 m) and a solid cylinder of nylon (0.4 m). c) Pressure port constructed for the top of the Pulse Tube to allow the pore fluid pressure of the sediment sample to be varied independently of the confining pressure.

Figure 5. a) Experimental and theoretical transmission coefficient spectra for a quartz sand sample in a copper jacket of length 0.2030 m (Dataset N/17/10/94/08) at a differential pressure of 1.379 MPa (200 psi). The best fit theoretical model ($R^2 = 0.71$) over the frequency bandwidth from 0.94 kHz to 8.44 kHz has a Stoneley wave velocity of 1780 ± 29 ms^{-1} and attenuation (Q^{-1}) of 0.016 ± 0.010 ($Q = 60$). b) Experimental and theoretical transmission coefficient spectra for quartz sand in a 0.385 m PVC container at 2.068 MPa (300 psi) differential pressure (Dataset 6/6/95/006). The best fit theoretical model ($R^2 = 0.90$) over the frequency bandwidth from 1.4 - 7.4 kHz has a Stoneley wave velocity of 1760 ± 15 ms^{-1} and attenuation (Q^{-1}) of 0.00667 ± 0.00340 ($Q = 150$).

Figure 6. Compressional wave velocity versus differential pressure for quartz sand in PVC and Copper jackets both a) without and b) with acoustic jacket corrections according to equation (16). The data point at 0 MPa is the average P-wave velocity of ten sands of similar porosity, corrected to the temperature, salinity and frequency of the Pulse Tube experiments, published by Shumway (1960) (see Table 3).

Figure 7. Compressional wave attenuation (Q_p^{-1}) versus differential pressure for quartz sand in PVC and Copper jackets both a) without and b) with acoustic jacket corrections according to equation (14). The data point at 0 MPa is the average P-wave attenuation of ten sands of similar porosity published by Shumway (1960) (see Table 3).

Figure 8. Statistical analysis of P-wave a) velocity and b) attenuation versus differential pressure for the combined data for quartz sand in PVC and copper jackets. See text for details.

Figure 9. Stages in the preparation of the copper jacketed silty-clay sediment samples: a) copper tube formed on mandrel with copper disc soldered on one end with a pore fluid port; b) copper jacket inside steel tube with ends folded back; c) sediment-filled tube with rubber diaphragm in place, sealed with white silicone; d) completed copper-jacketed silty-clay sample; e) photograph of a newly-opened silty-clay core.

Figure 10. Experimental and theoretical transmission coefficient spectra for silty clay sample 206C3 in a 0.424 m copper jacket at 2.068 MPa (300 psi) differential pressure (Dataset 26/9/97/933). The best fit theoretical model ($R^2 = 0.93$) over the frequency bandwidth from 1.4 kHz to 7.8 kHz has a Stoneley wave velocity of 1425 ± 17 ms^{-1} and attenuation (Q^{-1}) 0.0227 ± 0.0010 (Q = 44).

Figure 11. Ratio of the ultrasonic data from the cores to the Pulse Tube compressional wave velocities for silty-clay samples (corrected to 20 ºC, 500 kHz and 0 MPa pore water pressure).

Figure 12. Comparison of Pulse Tube compressional wave attenuation (Q_p^{-1}) versus sediment mean grain size (log scale) with seafloor data from Hamilton (1972).

List of Tables

1

Experimental observations									
Material	Sample length	Sample density	Confining pressure	Temperature	Pulse Tube Stoneley wave data			Frequency bandwidth	Ultrasonic P-wave Velocity at 0.5 MHz
					Velocity	Q^{-1}	Q		
	m	$Kg.m^{-3}$	MPa	ºC	ms^{-1}			kHz	ms^{-1}
Nylon	0.2014	1145	1.379	4	2400 ± 25	0.0067 ± 0.0038	149	1.0 – 8.0 kHz	2540 ± 19
PVC	0.4147	1382	2.413	4	2200 ±25	0.0280 ± 0.0042	36	1.6 – 9.0 kHz	2363 ±19

Values calculated from experimental data						
Material	Compressional wave data from Pulse Tube			Average frequency	Compressional wave velocities at 0.5 MHz	
	Velocity	Q^{-1}	Q		Pulse Tube velocity corrected for frequency dispersion	Ultrasonic measurement at 0.5 MHz
	ms^{-1}			kHz	ms^{-1}	ms^{-1}
Nylon	2500 ±25	0.071 ± 0.0038	140	4.5	2527 ± 29	2540 ±19
PVC	2309 ±25	0.0310 ±0.0042	32	5.3	2365 ± 29	2363 ± 19

2

3 Table 1. Acoustic properties of nylon and PVC from Pulse Tube and ultrasonic measurements.

4

Description	[1]Mean diameter	[1]Mean diameter	[1]Phi deviation	Sorting
Coarse sand	mm	phi units	phi units	Well sorted – phi deviation less than 0.5 phi
	1.97	-0.98	0.48	

Grain shape	[2]Particle Specific gravity	Wet density kgm^{-3}	Fractional porosity	[2]Mineralogy %	Pore water salinity parts per thousand
Sub-angular to rounded	2.65	2070	0.352	Quartz: 99.72% Alumina,Titania, Iron Magnesium all less than 0.1%	0

[1] Determined by manual measurement of 300 grains & converted to cumulative distribution by weight to calculate mean phi diameter ($= ½ (\varphi_{84} + \varphi_{16})$) and phi deviation ($=½(\varphi_{84} – \varphi_{16})$); φ_{16} and φ_{84} are the 16 and 84 percentiles.

[2] Data from the technical sheet for this sand published by the suppliers, Garside Sands, Leighton Buzzard, UK.

Table 2. Physical properties of the Leighton Buzzard quartz sand.

Experimental observations on sands from Shumway (1960)									Derived data: P-wave velocity adjusted to 5 kHz, 4 ºC, salinity 0 ppt (parts per thousand) and 2.413 MPa pore water pressure
Sample Number	Fractional porosity	Density	[1]Salinity	Temperature	Frequency	P-wave velocity	Q_p^{-1}	Q_p	
		$kg\ m^{-3}$	ppt	ºC	kHz	ms^{-1}			ms^{-1}
SD41a	0.388	1995	35	22.0	23.435	1735	0.0371	26.9	1594
SD38a	0.391	1990	35	22.4	26.076	1710	0.0334	30.0	1566
SD38b	0.393	2000	35	23.4	26.470	1725	0.0250	40.0	1587
SD41b	0.362	1990	35	22.0	23.335	1712	0.0322	31.0	1583
SD44a	0.383	2020	35	22.1	26.851	1748	0.0204	49.1	1619
SD44b	0.397	2030	35	22.6	26.949	1748	0.0247	40.6	1620
SD49b	0.357	1990	35	22.2	26.547	1725	0.0208	48.1	1600
SD52b	0.376	2050	35	22.9	27.032	1756	0.0191	52.4	1627
SD53a	0.387	2000	35	22.5	27.013	1760	0.0157	63.8	1636
SD53b	0.394	2000	35	22.6	26.925	1760	0.0157	63.9	1638
Average	0.383					1738	0.0244		1607
Std Dev	0.014					19	0.0076		24.5

[1]Salinity of the samples not published. Assumed to be the standard 35 parts per thousand of seafloor samples.

Table 3. Physical and acoustic properties of ten sands from Shumway (1960).

Experimental observations									**Derived data**			
Sample number	Porosity	Mean grain size (micron)	Density ($kg.m^{-3}$)	Pulse Tube data at 0.689 MPa differential pressure, 6 ºC & 5 kHz		Pulse Tube data at 2.068 MPa differential pressure, 6 ºC & 5 kHz		Ultrasonic data at 0 MPa, 20 ºC & 0.5 MHz	Pulse Tube data at 0.689 MPa adjusted to 0 MPa pore fluid pressure, 20 ºC & 0.5 MHz		Pulse Tube data at 2.068 MPa adjusted to 0 MPa pore fluid pressure, 20 ºC & 0.5 MHz	
				P-wave velocity (ms^{-1})	Q_p^{-1}	P-wave velocity (ms^{-1})	Q_p^{-1}	P-wave velocity (ms^{-1})	P-wave velocity (ms^{-1})	Ratio of ultrasonic to (adjusted) Pulse Tube velocity)	P-wave velocity (ms^{-1})	Ratio of ultrasonic to (adjusted) Pulse Tube velocity)
206C3	0.639	26.3	1650	1438	0.0176	1454	0.0236	1530	1518	1.008	1549	0.988
241A3LH	0.618	28.8	1687	1460	0.0208	1439	0.0217	1525	1549	0.984	1532	0.996
240A3LH	0.574	36.9	1766	1440	0.0298	1450	0.0373	1498	1565	0.957	1581	0.947
240A3UH	0.589	83.8	1721	1506	0.0174	1487	0.0190	1626	1585	1.026	1572	1.034
206B3LH	0.627	25.0	1627	1479	0.0243	1481	0.0261	1516	1574	0.963	1582	0.958
240C3	0.541	31.9	1826	1536	0.0136	1538	0.0130	1703	1609	1.059	1609	1.059
241A3UH	0.567	51.5	1779			1408	0.0149	1538			1534	1.003
240B3	0.633	32.0	1661			1450	0.0222	1531			1552	0.987
234B3UH	0.568	22.6	1778			1446	0.0222	1546			1549	0.998

Table 4. Physical and acoustic properties of the silty-clay samples.

Experimental observations on silty clays from Shumway (1960)									**Derived data**: P-wave velocity adjusted to 5 kHz, 6 ºC, 35 ppt salinity and 1.034 MPa pore water pressure
Sample Number	Fractional porosity	Density	[1]Salinity	Temperature	Frequency	P-wave velocity	Q_p^{-1}	Q_p	
		kg m^{-3}	Parts per thousand	ºC	kHz	ms^{-1}			ms^{-1}
SD35a	0.645	1600	35	19	23.051	1496	0.0139	72.0	1449
SD35b	0.605	1650	35	18.9	23.038	1512	0.0132	76.0	1464
SD35c	0.579	1670	35	19.1	23.360	1512	0.0204	49.1	1476
SD40a	0.630	1640	35	21	23.286	1510	0.0118	84.9	1460
SD40b	0.604	1620	35	21	23.214	1514	0.0173	57.8	1472
SD47a	0.578	1690	35	21.5	23.457	1530	0.0239	41.9	1469
SD47b	0.577	1700	35	21.5	23.441	1525	0.0281	36.0	1460
SD51a	0.600	1650	35	20.7	23.344	1521	0.0202	49.4	1465
AO8	0.604	1670	35	26.4	23.263	1551	0.0176	56.8	1485
PP6	0.604	1680	35	27.4	27.283	1559	0.0190	52.5	1487
CB9a	0.634	1597	35	23.9	23.861	1545	0.0194	51.6	1482
CB10	0.622	1645	35	23.6	23.329	1518	0.0096	104.5	1463
Mean	0.607					1524	0.0179		1469
Standard deviation	0.022					18.7	0.0052		11.5

[1]Salinity of the samples not published. Assumed to be the standard 35 parts per thousand of seafloor samples.

Table 5. Physical and acoustic properties of twelve silty-clays from Shumway (1960).

1
2

1

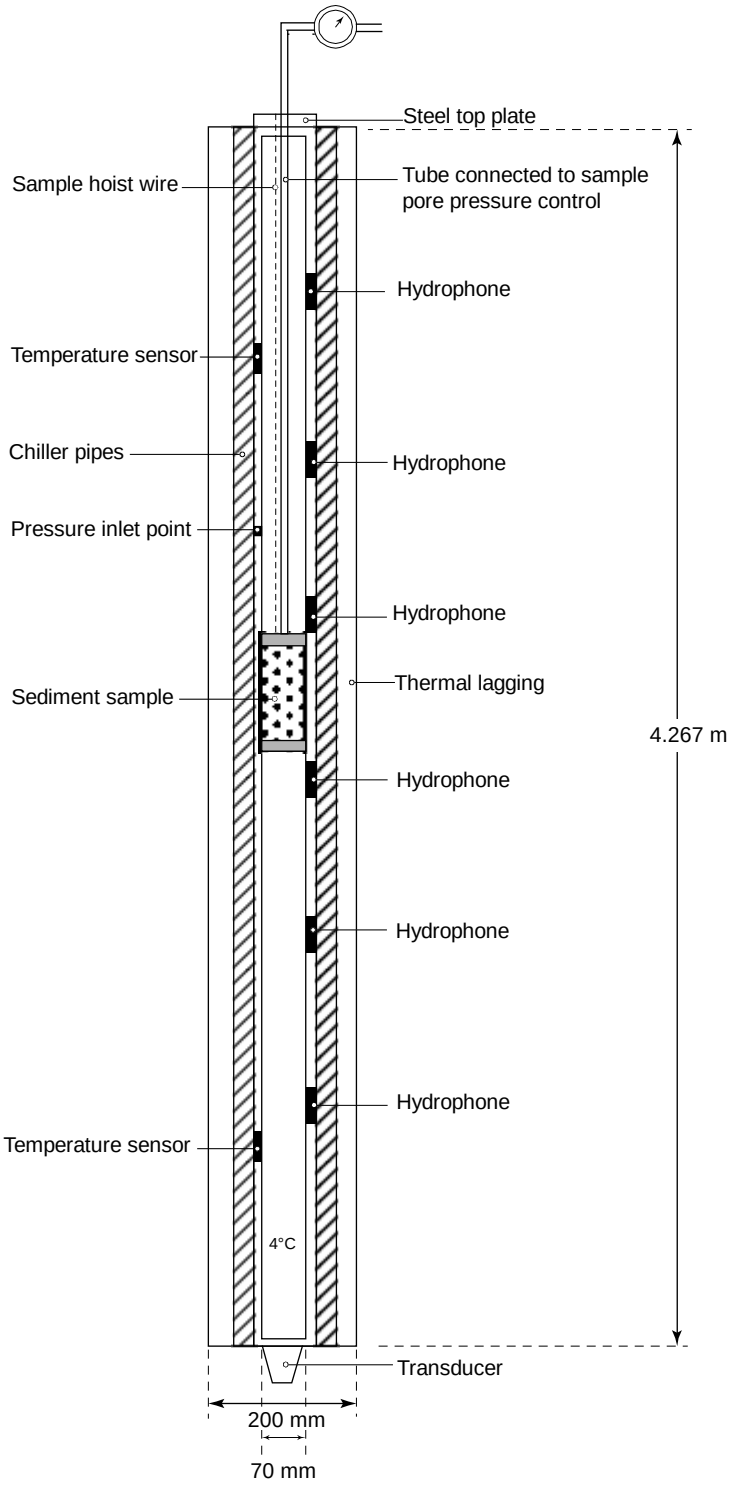

Figure 1. Schematic diagram of the acoustic Pulse Tube.

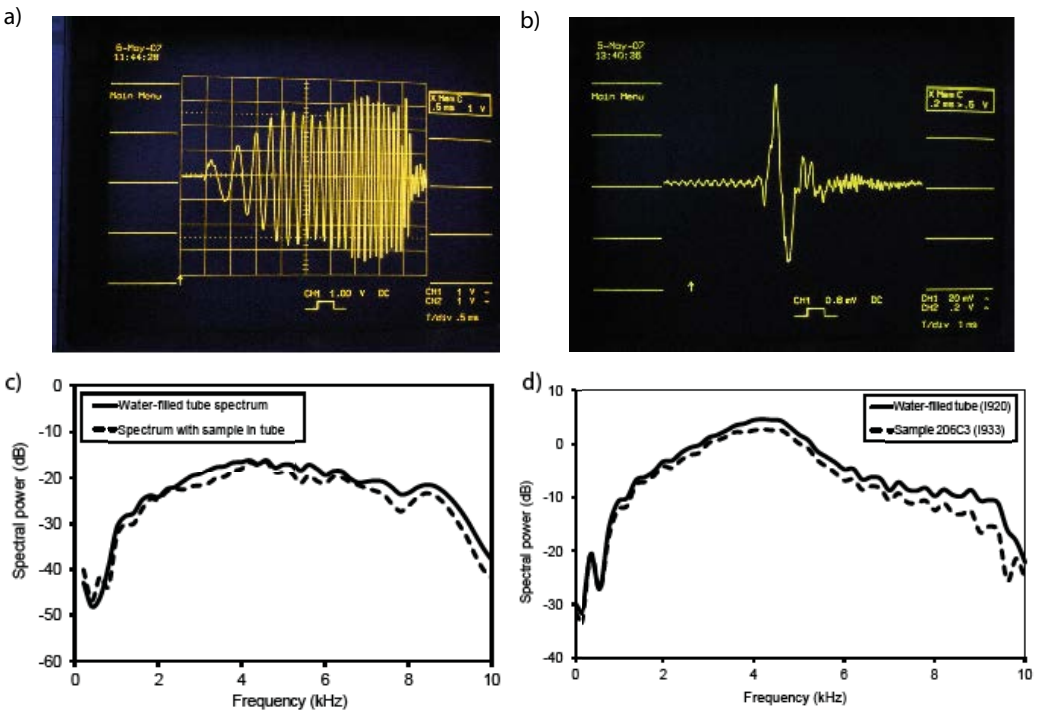

Figure 2. Oscilloscope screen images of (a) CHIRP and (b) impulse source pulses. Power spectra of the (c) CHIRP and (d) impulse sources pulses with and without a sample in the Pulse Tube.

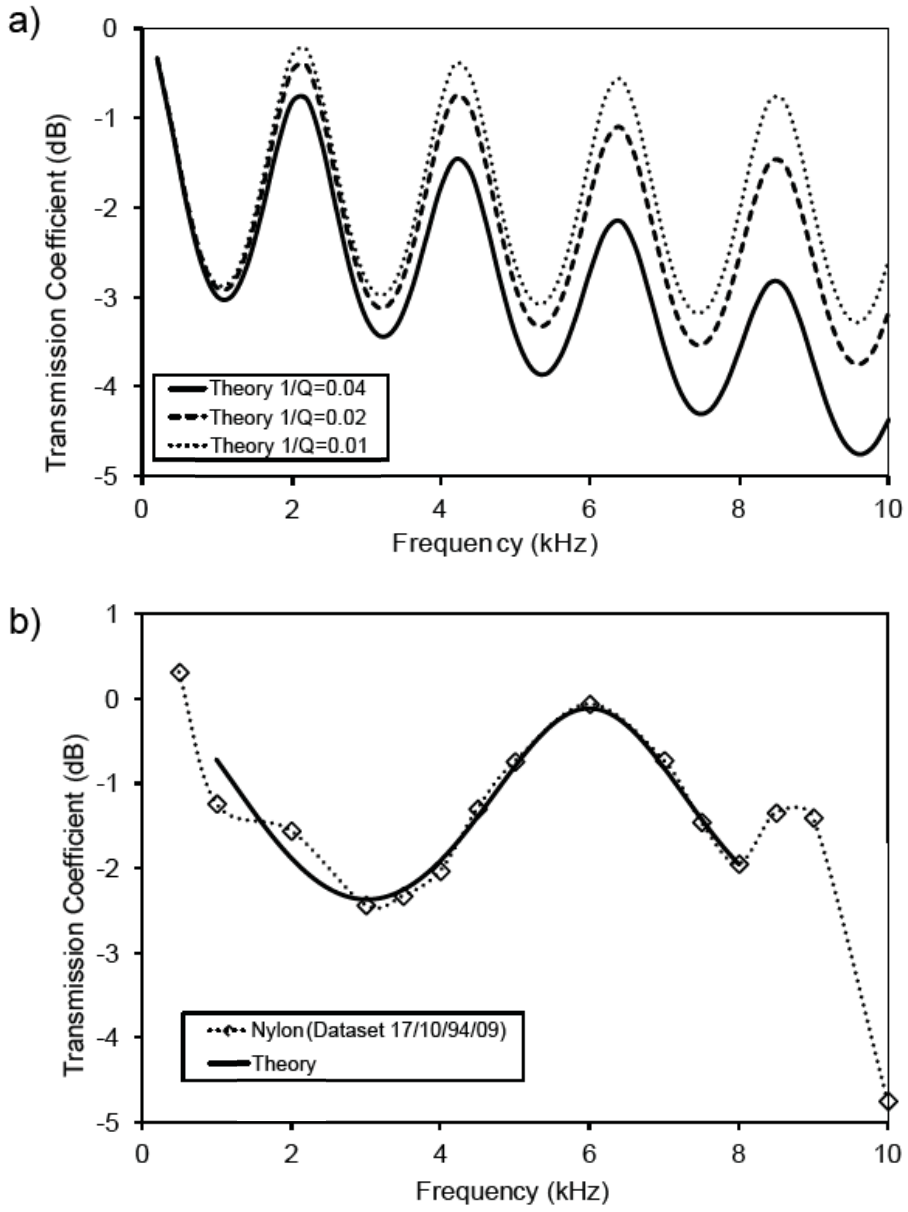

Figure 3. a) Theoretical transmission coefficient spectra for a quartz sand of length 0.4 m, Stoneley wave velocity 1700 $m.s^{-1}$ and density 2000 $kg.m^{-3}$. b) Experimental transmission coefficient spectrum for a 0.2014 m nylon cylinder (Dataset 17/10/94/09) at a confining pressure of 1.379 MPa (200 psi), with the best-fit theoretical solution (solid line) in the bandwidth 1 - 8 kHz. The Stoneley wave velocity and attenuation (Q^{-1}) for this solution (R^2 =0.92) are 2400 ± 25 ms^{-1} and 0.0067 ± 0.0038 (Q = 150) respectively.

a)

b)

c)

Figure 4. a) Photograph of typical grains of the well-sorted, quartz (Leighton Buzzard) sand of mean diameter 2 mm used to test the Pulse Tube measurement technique. b) Various samples prepared for the Pulse Tube. From left to right: three containers of sediment with jackets made of PVC (0.2 m), copper (0.2 m) and copper (0.4 m), a solid cylinder of PVC (0.4 m), a PVC jacketed sediment (0.4 m) and a solid cylinder of nylon (0.4 m). c) Pressure port constructed for the top of the Pulse Tube to allow the pore fluid pressure of the sediment sample to be varied independently of the confining pressure.

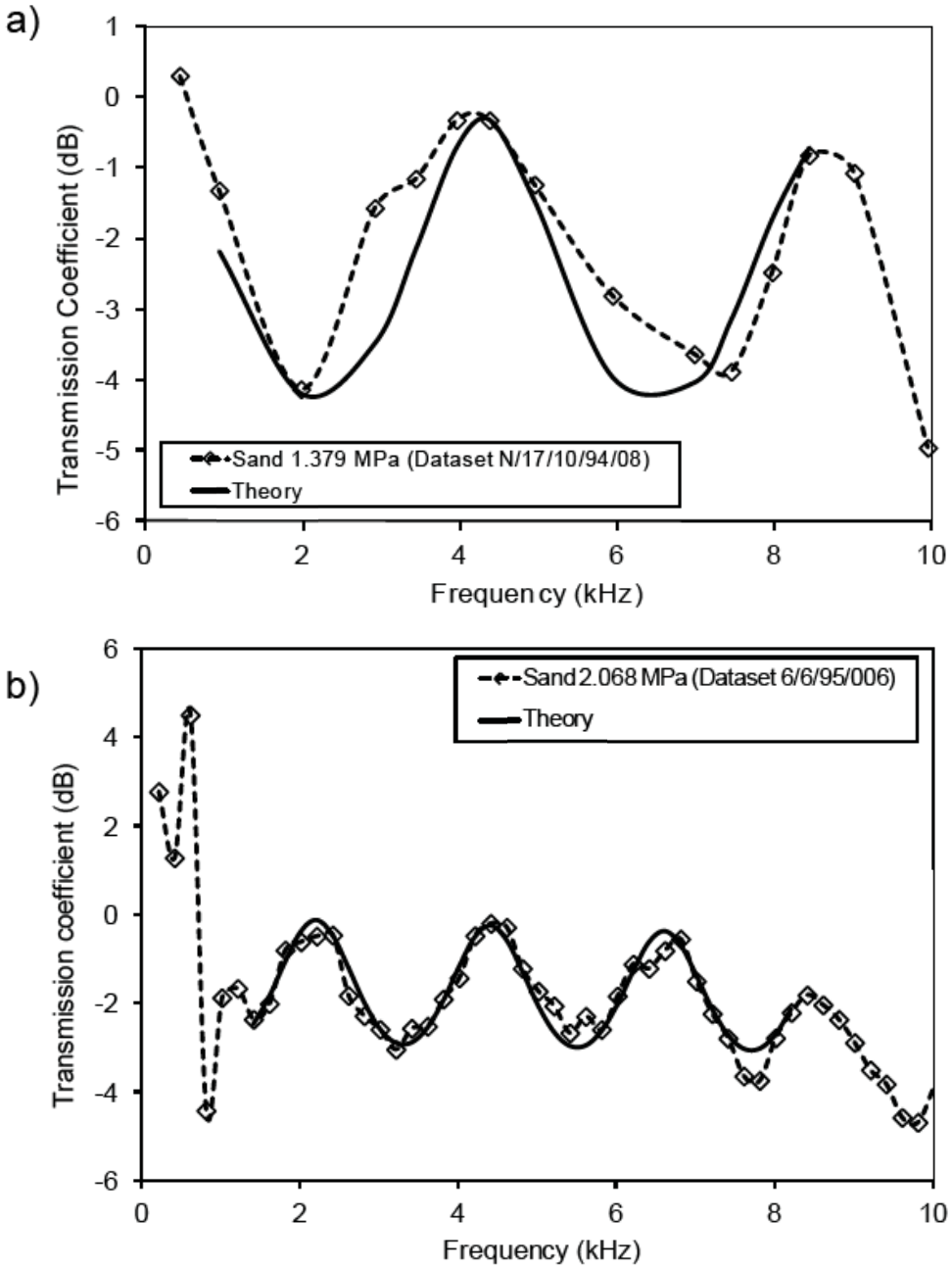

Figure 5. a) Experimental and theoretical transmission coefficient spectra for a quartz sand sample in a copper jacket of length 0.2030 m (Dataset N/17/10/94/08) at a differential pressure of 1.379 MPa (200 psi). The best fit theoretical model ($R^2 = 0.71$) over the frequency bandwidth from 0.94 - 8.44 kHz has a Stoneley wave velocity of 1780 ± 29 ms^{-1} and attenuation (Q^{-1}) of 0.016 ± 0.010 (Q = 60). b) Experimental and theoretical transmission coefficient spectra for quartz sand in a 0.385 m PVC container at 2.068 MPa (300 psi) differential pressure (Dataset 6/6/95/006). The best fit theoretical model ($R^2 =$ 0.90) over the frequency bandwidth from 1.4 - 7.4 kHz has a Stoneley wave velocity of 1760 ± 15 ms^{-1} and attenuation (Q^{-1}) of 0.00667 ± 0.00340 (Q = 150).

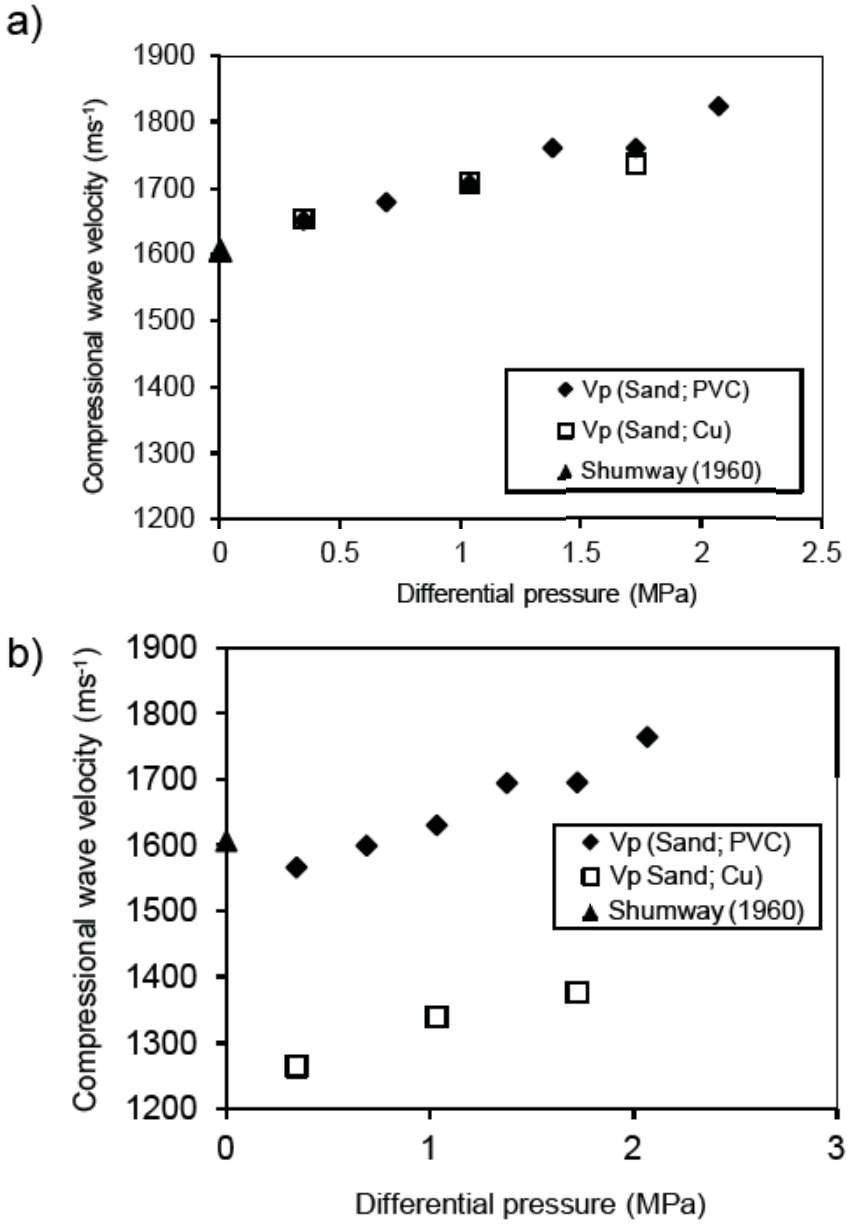

Figure 6. Compressional wave velocity versus differential pressure for quartz sand in PVC and Copper jackets both a) without and b) with acoustic jacket corrections according to equation (16). The data point at 0 MPa is the average P-wave velocity of ten sands of similar porosity, corrected to the temperature, salinity and frequency of the Pulse Tube experiments, published by Shumway (1960) (see Table 3).

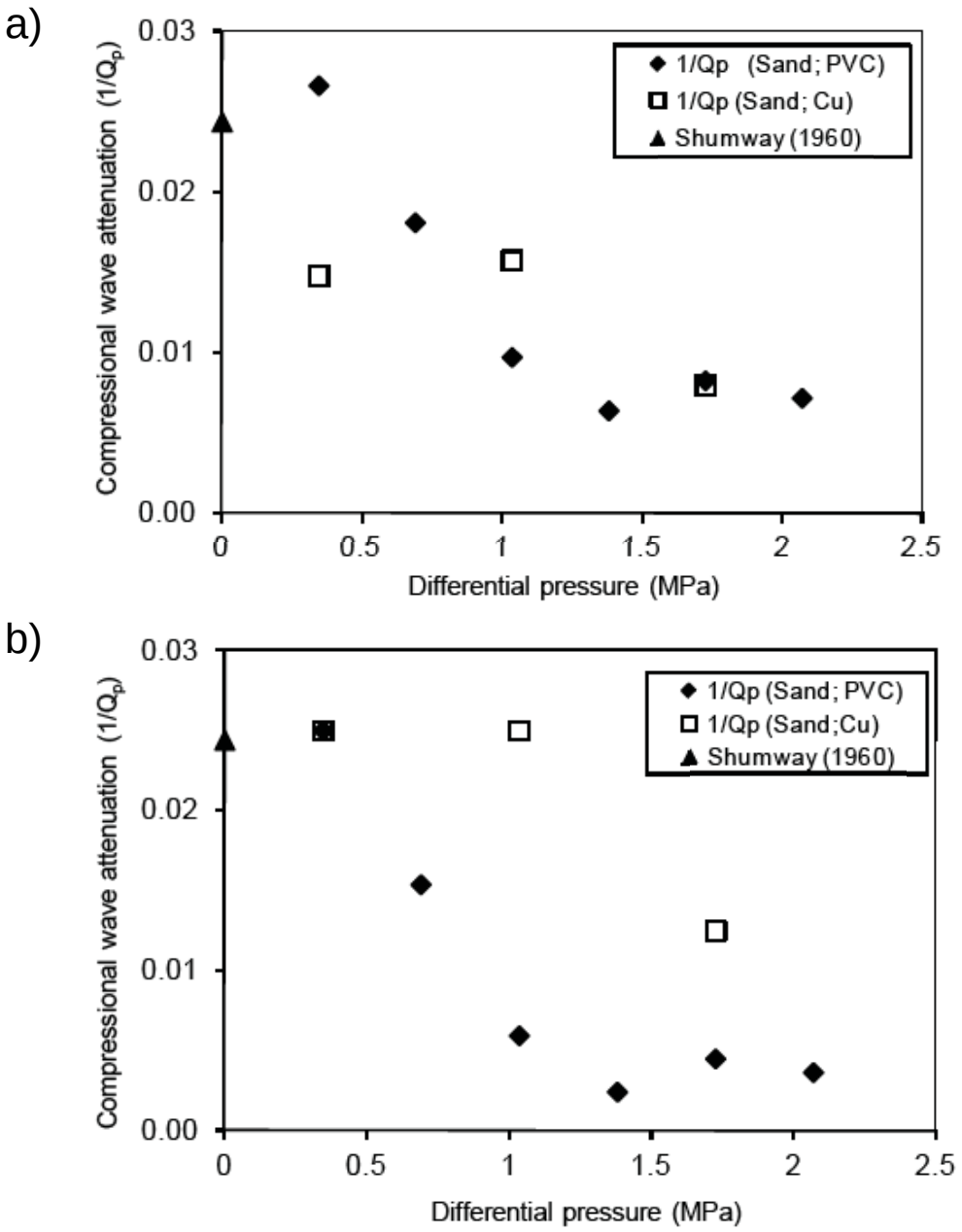

Figure 7. Compressional wave attenuation (Q_p^{-1}) versus differential pressure for quartz sand in PVC and Copper jackets both a) without and b) with acoustic jacket corrections according to equation (14). The data point at 0 MPa is the average P-wave attenuation of ten sands of similar porosity published by Shumway (1960) (see Table 3).

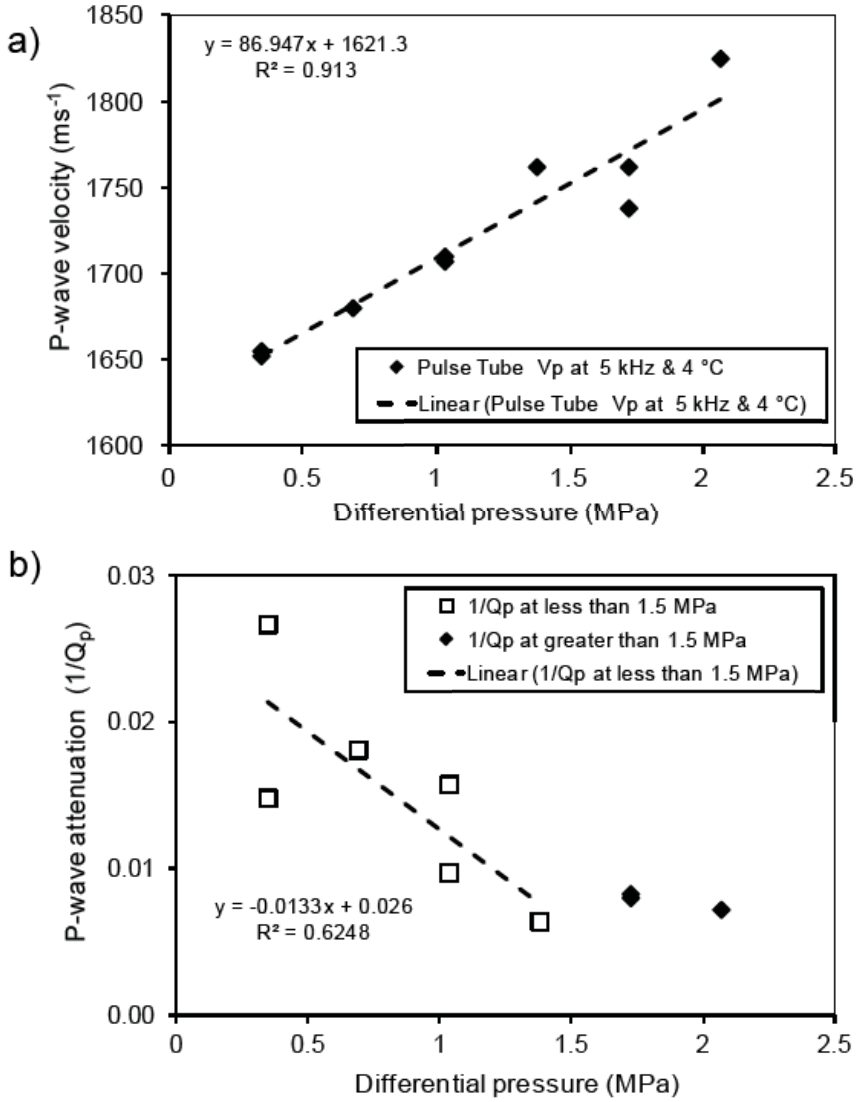

Figure 8. Statistical analysis of P-wave a) velocity and b) attenuation versus differential pressure for the combined data for quartz sand in PVC and copper jackets. See text for details.

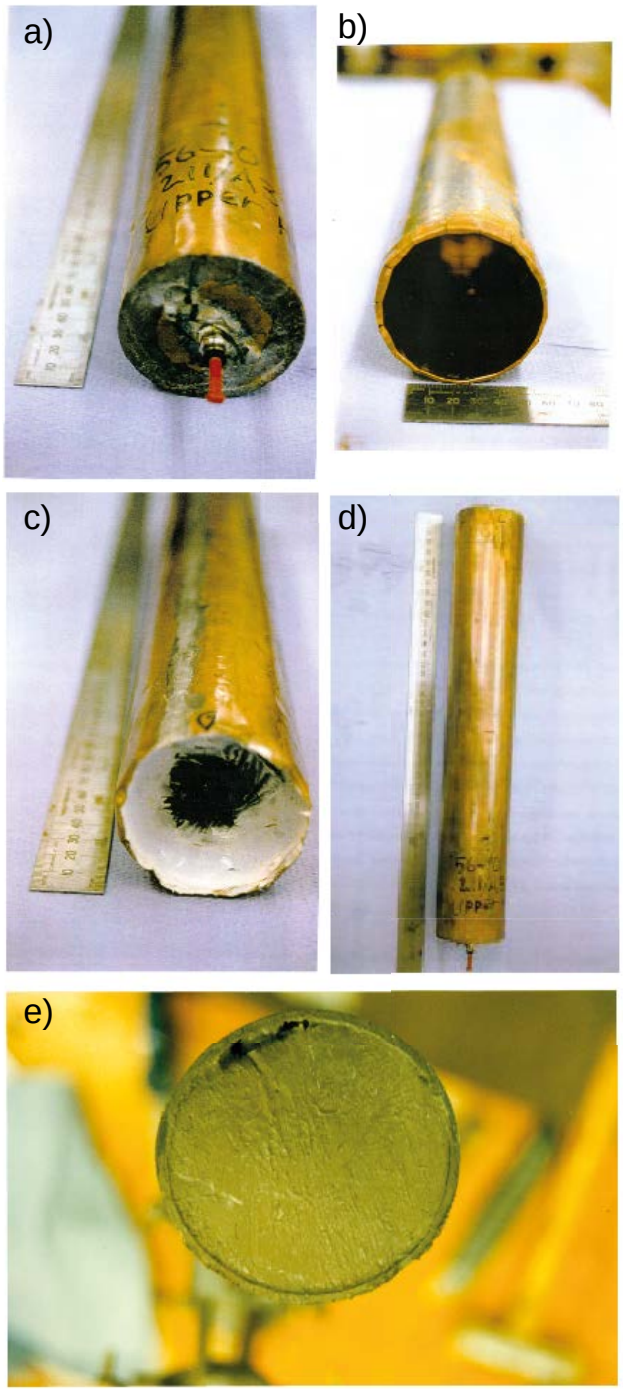

Figure 9. Stages in the preparation of the copper jacketed silty-clay sediment samples: a) copper tube formed on mandrel with copper disc soldered on one end with a pore fluid port; b) copper jacket inside steel tube with ends folded back; c) sediment-filled tube with rubber diaphragm in place, sealed with white silicone; d) completed copper-jacketed silty-clay sample; e) photograph of a newly-opened silty-clay core.

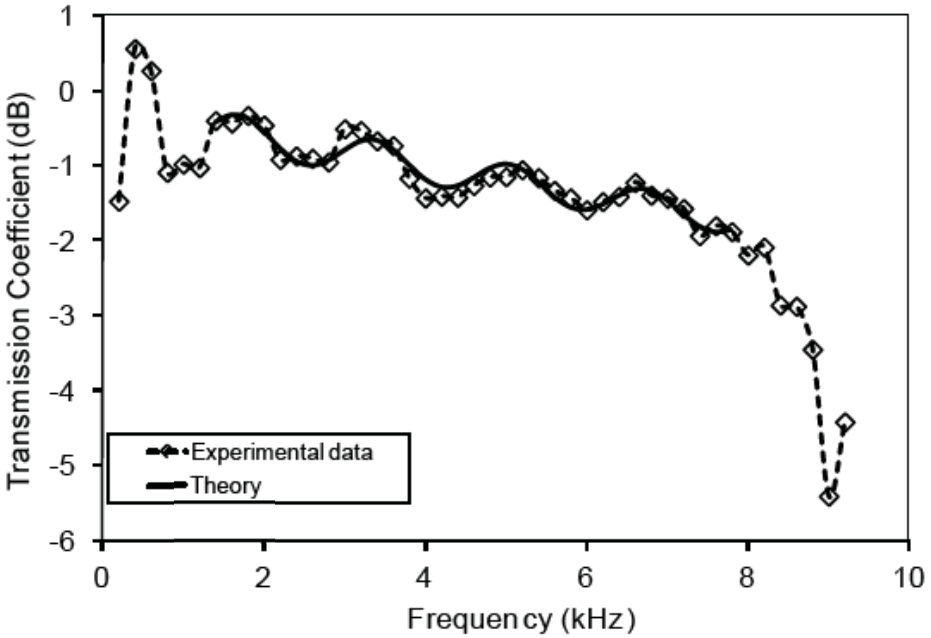

Figure 10. Experimental and theoretical transmission coefficient spectra for silty clay sample 206C3 in a 0.424 m copper jacket at 2.068 MPa (300 psi) differential pressure (Dataset 26/9/97/933). The best fit theoretical model (R^2 = 0.93) over the frequency bandwidth from 1.4 kHz to 7.8 kHz has a Stoneley wave velocity of 1425 ± 17 ms^{-1} and attenuation (Q^{-1}) 0.0227 ± 0.0010 (Q = 44).

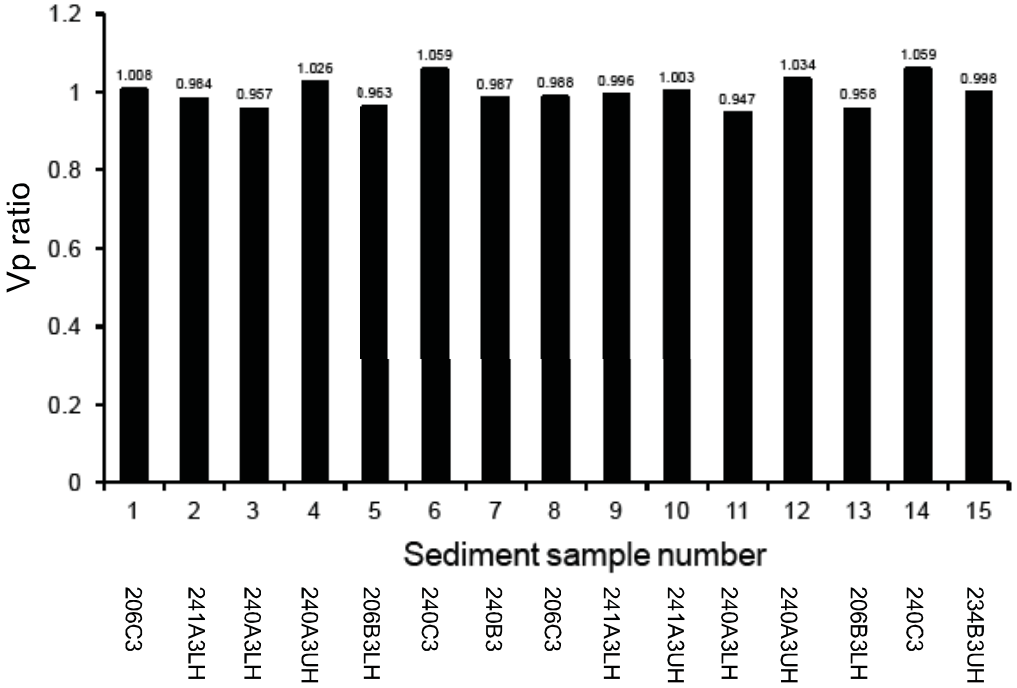

Figure 11. Ratio of the ultrasonic data from the cores to the Pulse Tube compressional wave velocities for silty-clay samples (corrected to 20 ºC, 500 kHz and 0 MPa pore water pressure).

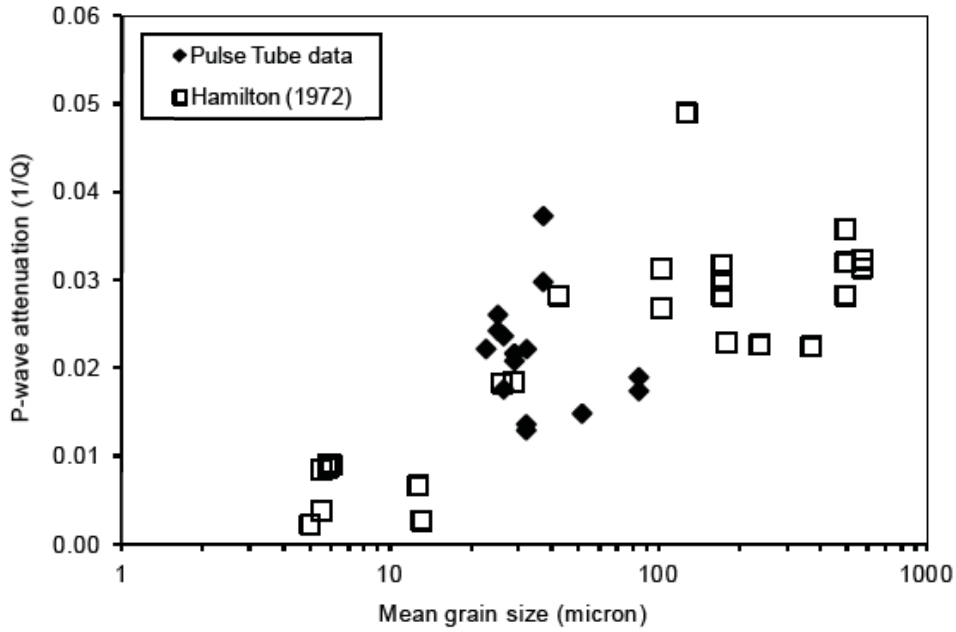

Figure 12. Comparison of Pulse Tube compressional wave attenuation (Q_p^{-1}) versus sediment mean grain size (log scale) with seafloor data from Hamilton (1972).